

of correlation energy effects. The first type, the so-called non-dynamic correlation, is associated with the breaking down of the Hartree-Fock model in the regions of the potential surface where we have degeneracy or near-degeneracy of several configurations. This frequently occurs in reactivity problems when we describe the rupture and formation of bonds. This problem can be solved with the MCSCF method with a limited CI expansion that includes the near-degenerate configurations. Unfortunately this approach is not capable of describing satisfactorily the second type of correlation effect, i.e., the dynamic correlation associated with the motion of electrons. To take this contribution into account, a large CI expansion is required. Nevertheless, for similar structures, like those we have found in the transition-state region, it is quite conceivable to assume that this contribution does not change very much. Thus, reliable information can be obtained by comparing these various structures (intermediates and transition states) and evaluating the relative energy barriers. These considerations also suggest that improvement in the correlation treatment should not change the qualitative nature of the potential surface. The situation is quite different when we consider the product molecules or the reactant molecules, and we try to compare them with the transition-state region. The contribution of the dynamic correlation in these three different situations will be

in general quite different. Because of this, care must be taken in evaluating at this computational level the exothermicities of the reaction or in comparing the activation energies computed at the MCSCF level (see the data reported in Table I) with the experimental results. The theoretical energy of activation is about 25 kcal/mol at the STO-3G level but becomes about 53 kcal/mol at the 4-31G level. This value is too high when compared with the value of the activation energy of 32 kcal/mol¹⁹ that can be estimated on the basis of the experimentally known gas-phase standard heats of formation of ketene, ethylene, and cyclobutanone.

Registry No. Ketene, 463-51-4; ethylene, 74-85-1.

Supplementary Material Available: Tables of optimized STO-3G and 4-31G geometrical parameters for various structures from the C1(∥) and C1(⊥) reaction paths (Tables II and III), STO-3G parameters for C2(⊥) and O(∥) reaction paths (Tables IV and V), STO-3G and 4-31G parameters for the supra-antara SOSP (Table VI), and STO-3G and 4-31G parameters for ethylene, ketene, cyclobutanone, and 2-methyleneoxatane (Table VII) (6 pages). Ordering information is given on any current masthead page.

Theoretical Interpretation of the Absorption and Ionization Spectra of the Paracyclophanes

Sylvio Canuto[†] and Michael C. Zerner*

Contribution from the Quantum Theory Project, University of Florida, Gainesville, Florida 32611. Received December 27, 1988

Abstract: The ultraviolet absorption spectra of the [*m*-*m*]paracyclophanes are studied by utilizing an INDO/S-CI method. The [4.4] and higher paracyclophanes can be considered as two parallel *p*-xylenes and the spectrum is interpreted as a simple doubling of the xylene bands. For the [3.3]paracyclophane the first band observed in absorption is assigned to the second excited state, ¹B_{3u}, but with the first calculated state, ¹B_{2g}, borrowing intensity from higher states. This lowest ¹B_{2g} state may be responsible for an inflection on the first observed band and it is held responsible for the emission observed in concentrated benzene solution. By utilizing di-*p*-xylene as a model system for the [*m*-*m*]paracyclophanes, the dependence of the ultraviolet absorption spectra with the interring separation is systematically analyzed. [2.2]Paracyclophane, known to have a short interring separation (3.1 Å) and a boat-like distortion of each ring, presents a spectrum that is considerably more complex. All seven bands observed experimentally are considered in our theoretical assignment (i.e. <60 000 cm⁻¹). Our calculations utilize the crystallographic structure and the results indicate that the lowest band consists of two transitions, one allowed (¹B_{3u}) and one forbidden (¹B_{2g}), borrowing intensity from a higher ¹B_{2u} state via the a_u vibrational mode (twisting of the rings in opposite directions around the major axis). This lowest state ¹B_{2g} is interpreted as responsible for the weak fluorescence and for the long axis polarized absorption. The observed phosphorescence of [2.2]paracyclophane is assigned to the emission ³B_{3g}-¹A_g. For the calculation of this emission energy the geometry of the excited ³B_{3g} state is optimized by using the ab initio SCF gradient technique with the STO-3G basis set. The ionization spectrum of the [2.2]paracyclophane is calculated by using both the INDO/S-CI method and the ab initio SCF procedure with a split-valence basis set. The interpretation of the spectrum of the paracyclophanes presented in this paper is perhaps the most consistent so far available and conforms very well with all known experimental characteristics.

1. Introduction

The interpretation of the electronic absorption and emission spectra of systems of cofacially arrayed molecular hydrocarbons is of great importance in understanding steric and transannular resonance effects, charge transfer, and the nature of the intermolecular interaction. Among these systems cyclophanes have been of particular interest.¹ In [*m*-*n*]cyclophanes two benzene rings are held together by bridges of (CH₂)_{*m*} and (CH₂)_{*n*}. Different inter-ring distances are associated with different values of *m* and *n*. The [*m*-*n*]cyclophanes thus provide a regular series of molecules in which the interaction of aromatic rings at varying

separations can be systematically examined. In the smaller cyclophanes the two benzene rings are so close as to give rise to abnormal absorption bands that cannot be traced back to the usual

- (1) (a) Cram, D. J.; Steinberg, H. J. *J. Am. Chem. Soc.* **1951**, *73*, 5691. (b) Brown, C. J. *J. Chem. Soc.* **1953**, 3265. (c) Koutecki, J.; Paldus, J. *Collect. Czech. Chem. Commun.* **1962**, *27*, 599. (d) Gleiter, R. *Tetrahedron Lett.* **1969**, *51*, 4453. (e) Boyd, R. H. *J. Chem. Phys.* **1968**, *49*, 2574. (f) Schweitzer, D.; Colpa, J. P.; Behnke, J.; Hansser, K. H.; Haenel, M.; Staab, H. A. *Chem. Phys.* **1975**, *11*, 373. (g) Schweitzer, D.; Colpa, J. P.; Hansser, K. H.; Staab, H. A. *J. Luminesc.* **1976**, *12/13*, 363. (h) Hoffman, R. *Acc. Chem. Res.* **1971**, *4*, 1. (i) Vogler, H. *Theor. Chim. Acta. (Berlin)* **1981**, *60*, 65. (j) Paddow-Row, M. N. *Acc. Chem. Res.* **1982**, *15*, 245. (k) Boekelheide, V. *Acc. Chem. Res.* **1980**, *13*, 65. (l) Voegtle, E.; Höhner, G. *Top. Curr. Chem.* **1978**, *74*, 1. (m) Hoffman, R.; Imamura, A.; Hehre, W. J. *J. Am. Chem. Soc.* **1968**, *90*, 1499.

* Permanent address: Departamento de Física, Universidade Federal de Pernambuco, 50000 Recife PE, Brazil.

$\pi\pi^*$ signature of benzene. For instance, in [2.2]paracyclophane the separation of the aromatic rings is shorter than those of benzene in solution and the experimental absorption spectrum of [2.2]paracyclophane exhibits bands of considerable interest.²⁻⁴ Additionally, X-ray analysis⁵ has established that in the structure of [2.2]paracyclophane each benzene ring is greatly distorted into a boat-like configuration.

Structural and spectroscopic investigations on paracyclophanes are widespread. Early comprehensive theoretical investigations on the electronic structure of these systems are those of Vala, Hillier, Rice, and Jortner⁶ and Hillier, Glass, and Rice.⁷ More recently, there has been a number of theoretical investigations directed to the interpretations of both the ultraviolet absorption^{8,9} and photoelectron^{8,10} spectra. In some instances, the theoretical results have been admittedly inadequate.⁸ On the basis of these studies, however, the intricacies of the absorption and emission spectra of $[m\cdot n]$ paracyclophanes are being sorted out. It is the aim of this study to further this understanding, and we examine the spectra of [2.2]-, [3.3]-, and [4.4]paracyclophanes. Higher order paracyclophanes, as we shall discuss, are easily understood in terms of the decreasing interaction between the molecular systems of rings. [2.2]Paracyclophane is far more interesting, exhibiting a greater degree of structural distortion, and an understanding of the absorption and emission spectra is more difficult. Consequently, for this system we have also performed geometry optimization of the ground and some low-lying excited states and these are reported elsewhere.¹¹ Even though the inter-ring distance seems to be the most clear geometrical parameter affecting the spectra of these systems, for some states of the [2.2]paracyclophane we have performed a full geometry optimization examining the possibility of twisting and tilting. Additionally, in the present paper, we also study the photoelectron spectrum of the [2.2]paracyclophane in order to understand in a complementary fashion the experimental features related to the interaction between the aromatic rings and the splitting of benzene π bands. Single-bridged cyclophanes have also attracted recent interests.^{12,13}

This study combines ab initio and semiempirical methods and these are described in the next section.

2. Methods of Calculations

The calculations of the ultraviolet absorption spectra of the $[m\cdot n]$ -paracyclophanes are performed with use of the INDO/S technique.¹⁴ The two-center Coulomb integrals are calculated by using the Mataga-Nishimoto expression, and the two-center resonance integrals depend on the scaling factors f_σ and f_π , as described earlier.¹⁵ In this paper we adopt $f_\sigma = 1.0$ and $f_\pi = 0.585$. After the SCF calculation, excited configurations are generated from single excitations and these are superimposed through a configuration interaction treatment to obtain the excited states. Oscillator strengths are calculated by using the dipole length operator.

(2) Iwata, S.; Fuke, K.; Sasaki, M.; Nagakura, S.; Otsubo, T.; Misumi, S. *J. Mol. Spectrosc.* **1973**, *46*, 1.

(3) Cram, D. J.; Allinger, N. L.; Steinberg, H. *J. Am. Chem. Soc.* **1954**, *76*, 6132.

(4) Fuke, K.; Nagakura, S.; Kobayashi, T. *Chem. Phys. Lett.* **1975**, *31*, 205.

(5) Hope, H.; Bernstein, I.; Trueblood, K. N. *Acta Crystallogr.* **1972**, *B28*, 1733.

(6) Vala, M. T.; Hillier, I. H.; Rice, S. A.; Jortner, J. *J. Chem. Phys.* **1966**, *44*, 23.

(7) Hillier, I. H.; Glass, L.; Rice, S. A. *J. Chem. Phys.* **1966**, *45*, 3015.

(8) Duke, C. B.; Lipari, N. O.; Salaneck, W. R.; Schein, L. B. *J. Chem. Phys.* **1975**, *63*, 1758.

(9) Wisor, A. K.; Czuchajowski, L. *J. Phys. Chem.* **1986**, *90*, 1541. See also: Czuchajowski, L.; Wisor, A. K. *J. Electron Spectrosc. Relat. Phenom.* **1987**, *43*, 169.

(10) Doris, K. A.; Ellis, D. E.; Ratner, M. A.; Marks, T. J. *J. Am. Chem. Soc.* **1984**, *106*, 2491.

(11) Canuto, S.; Zerner, M. C. *Chem. Phys. Lett.* **1989**, *157*, 353.

(12) Carballeira, L.; Casado, J.; Gomes, E.; Rios, M. A. *J. Chem. Phys.* **1982**, *77*, 5655.

(13) Rice, J. E.; Lee, T. J.; Remington, R. B.; Allen, W. D.; Clabo, D. A., Jr.; Schaeffer, H. F., III. *J. Am. Chem. Soc.* **1987**, *109*, 2902.

(14) Zerner, M. C.; Loew, G. H.; Kirchner, R.; Muller-Westerhoff, U. T. *J. Am. Chem. Soc.* **1980**, *102*, 589.

(15) Ridley, J.; Zerner, M. C. *Theor. Chim. Acta.* **1973**, *32*, 111.

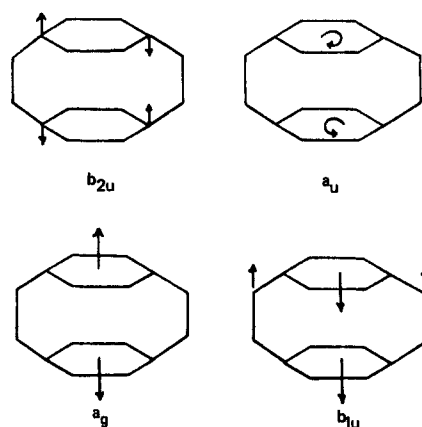


Figure 1. Some low-energy vibrational modes of [2.2]paracyclophane.

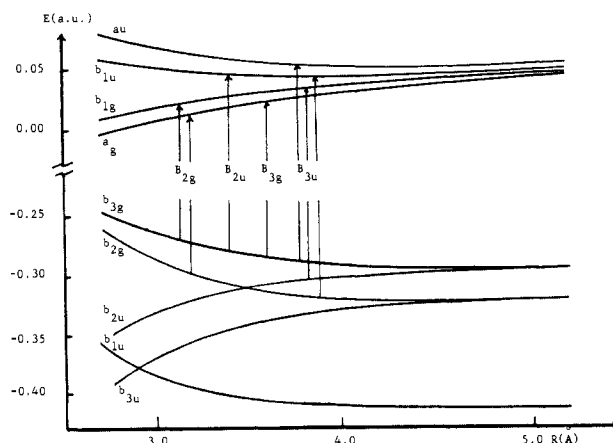


Figure 2. Molecular orbital energies of di-*p*-xylene as a function of the interplanar separation. The four lowest lying excited states and the corresponding excitations are indicated.

Table I. Comparison of Calculated and Experimental Absorption Spectrum of *p*-Xylene (All Energies in 1000 cm^{-1})

observed ^a		calculated			
energy	intensity	symmetry	energy	oscillator strength	description
36.4	weak	B ₃₁	36.3	0.017 <i>x</i>	benzene B _{2u}
45.2-47.8	medium	B _{2u}	45.9	0.158 <i>y</i>	benzene B _{1u}
51.5	strong	B _{3u}	51.2	0.768 <i>x</i>	benzene E _{1u}
52.1	strong	B _{2u}	51.8	0.808 <i>y</i>	benzene E _{1u}
		B _{1u}	52.8	0.000 <i>z</i>	
		A _u	53.8		
		B _{1u}	54.1	0.001 <i>z</i>	
		A _u	55.8		
		B _{1u}	55.9	0.002 <i>z</i>	
		B _{1u}	59.2	0.000 <i>z</i>	

^aReference 19, maximum values in EtOH.

In all calculations of the paracyclophanes the major *z* axis is directed perpendicular to the planes of the rings, *y* is parallel to the benzene long axis, and *x* is parallel to the short axis. In a forthcoming paper the molecular geometries are calculated at the ab initio SCF level in a minimal (STO-3G) basis set by using the GAMESS program.¹⁶ In this paper, the geometries are taken from the X-ray information, where available, and these are given later on in the next section.

The photoelectron spectrum of [2.2]paracyclophane is calculated at both the semiempirical INDO/S and ab initio Δ SCF levels of approximation. In the first scheme the configurations are generated with the SCF ground-state radical cation as the reference function. Naturally, this type of calculation may also be compared directly with the absorption spectrum of the radical cation. In the ab initio method the SCF energies of the neutral and cationic states are calculated separately and the ion-

(16) GAMESS; Dupuis, M.; Spangler, D.; Wendoloski, J.; NRCC Software Catalogue, 1980; Lawrence Berkeley Laboratory, USDOE; Program QG01.

Table IV. Comparison of Calculated and Experimental Absorption Spectrum of [3.3]Paracyclophane (All Energies in 1000 cm⁻¹) Calculated as Di-*p*-xylene with Inter-ring Separation of 3.30 Å (See Text for Further Details)

observed ^a energy	calculated		
	symmetry	energy	oscillator strength
34.0	B _{2g}	33.3	
	B _{3u}	35.6	0.013 <i>x</i>
37.3–39.2	B _{3g}	40.2	
	B _{2g}	43.4	
	B _{2u}	44.3	0.184 <i>y</i>
45.9	B _{3g}	44.8	
	B _{3u}	48.1	0.285 <i>x</i>
47.6	B _{2u}	49.0	0.080 <i>y</i>
>50.0	B _{1u}	50.7	0.001 <i>z</i>
	A _g	51.2	
	B _{3u}	51.5	0.522 <i>x</i>
	B _{2u}	52.2	0.766 <i>y</i>
	B _{2g}	52.9	
	B _{3g}	53.7	
	A ₁	53.8	
	B _{1g}	54.1	
	B _{1u}	54.5	0.006 <i>z</i>
	A _g	54.8	
	A _u	55.1	
	B _{1g}	55.3	
	B _{3u}	56.2	0.731 <i>x</i>
	B _{1u}	56.5	0.001 <i>z</i>
	A _u	56.7	
	B _{1u}	56.7	0.000 <i>z</i>
	A _g	57.0	
	B _{1g}	57.0	
	B _{2u}	57.8	1.220 <i>y</i>
	A _g	58.3	
	B _{2g}	58.5	
	B _{3g}	60.0	
	A _u	60.0	

^a Reference 3.

boat-like deformation, but the calculations on the [2.2]paracyclophane showed only small shifts of the calculated spectrum as compared to the idealized structure with parallel rings. Thus we consider this minor tendency to form boats as inconsequential for the positioning of the excited states. Also we consider this lateral displacement of the [3.3]paracyclophane as a likely result of packing forces. Therefore, we have idealized the structure of the [3.3]paracyclophane with two parallel xylene molecules at the 3.30-Å separation. Calculations with the observed structure do not differ much from this model, and we consider the model calculation somewhat more appropriate for comparison with the solution spectrum examined below.

The calculated results for this model are presented along with those obtained from experiment in Table IV. A ¹B_{2g} state is calculated to lie at 33 300 cm⁻¹ in good agreement with the first band observed in 95% ethanol by Cram, Allinger, and Steinberg³ at 34 000 cm⁻¹. However, as this observed peak has the shape characteristic of allowed bands it seems more natural to assign it to the allowed ¹B_{3u} state calculated as the second state at 35 600 cm⁻¹. The lowest ¹B_{2g} state would contribute to the peak intensity at 34 000 cm⁻¹ with vibronic coupling via the b_{1u} vibrational mode (Figure 1) or perhaps be attributed to an inflection appearing at ~32 000 cm⁻¹. This lowest ¹B_{2g} state should be the one responsible for the fluorescence at 31 800 cm⁻¹ from concentrated benzene solution in which the expected interring separation of 3.35 Å is very close to that of [3.3]paracyclophane.²¹

Three transitions are observed between 37 300 and 39 200 cm⁻¹, and it might be tempting to collate these with the fingerprint-like ¹B_{3u} state of the xylene spectrum observed in this region. As this state has already been assigned to the broad peak at 34 000 cm⁻¹ this leaves the assignment of these bands at ~37 300, ~38 500, and ~39 200 cm⁻¹ to one ¹B_{3g}, one ¹B_{2g}, and one ¹B_{2u} calculated

Table V. Comparison of Calculated and Experimental Absorption Spectrum of [2.2]Paracyclophane (All Energies in 1000 cm⁻¹) (See Text for Details)

observed ^a			calculated		
energy	oscillator strength	description	symmetry	energy	oscillator strength
(I) 32.8	0.001	(30.4–30.7) max ^b	B _{2g}	30.3	
		0–0 ^c	B _{3u}	33.6	0.029 <i>x</i>
(II) 35.2	0.003	differently polar.	B _{3g}	36.0	
(III) 39.0–41.0	0.050	<i>x</i> or <i>z</i> polar.	B _{2u}	40.3	0.122 <i>y</i>
			B _{2g}	40.3	
			B _{3g}	42.4	
(IV) 44.5	0.260	<i>x</i> or <i>z</i> polar.	B _{3u}	44.4	0.082 <i>x</i>
			B _{2u}	45.2	0.082 <i>y</i>
			A _g	46.1	
			B _{1u}	46.8	0.000 <i>z</i>
(V) 48.7	0.121	<i>x</i> or <i>z</i> polar.	B _{3g}	47.4	
			B _{3u}	47.9	0.677 <i>x</i>
			B _{2g}	49.7	
			B _{1u}	49.8	0.002 <i>z</i>
(VI) 53.0	1.070		B _{2u}	50.2	0.877 <i>y</i>
			A _u	51.4	
			A _g	51.8	
			B _{1g}	53.1	
			A _u	53.2	
			B _{1u}	53.4	0.004 <i>z</i>
			B _{1g}	53.8	
			A _u	54.1	
			A _g	54.2	
			B _{1g}	54.6	
			B _{1u}	55.2	0.001 <i>z</i>
			B _{2u}	56.2	0.000 <i>y</i>
			B _{3u}	57.1	0.610 <i>x</i>
			A _g	57.5	
(VII) 57.8	0.020		B _{3g}	58.4	
			B _{2u}	58.8	0.652 <i>y</i>
			B _{2g}	59.2	
			B _{1u}	59.5	0.033 <i>z</i>
			A _g	60.1	
			A _u	60.3	

^a Reference 2 unless otherwise indicated. ^b Maximum value in *n*-heptane at room temperature. ^c Reference 22. 0–0 transition in crystal.

between 40 200 and 44 300 cm⁻¹. The transition observed at ~45 900 cm⁻¹ is then assigned to the ¹B_{3g} calculated at 44 800 cm⁻¹ and the allowed ¹B_{3u} calculated at 48 100 cm⁻¹, and that observed at 47 600 cm⁻¹ to two states calculated at 49 000 cm⁻¹ (¹B_{2u}) and 50 700 cm⁻¹ (¹B_{1u}). The observed spectrum also shows evidence of a strong peak starting around 50 000 cm⁻¹. In this region we calculate several states and some with considerable intensity such as the ¹B_{3u} at 51 500 cm⁻¹ and ¹B_{2u} at 52 200 cm⁻¹.

D. [2.2]Paracyclophane. The singlet absorption spectrum of [2.2]paracyclophane was measured by Iwata, Fuke, Sasaki, Nagakura, Otsubo, and Misumi² in *n*-heptane solution at room temperature (below 49 000 cm⁻¹) and in 3-methylpentane glass at 77 °K (above 49 000 cm⁻¹). They have also measured the polarized spectrum of the single crystal at room temperature. Their results support and extend those obtained by Cram, Allinger, and Steinberg³ for the solution spectrum and by Ron and Schnepf^{22,23} for the single crystal. Fuke, Nagakura, and Kobayashi⁴ later reported the two-photon absorption spectrum of [2.2]paracyclophane. Theoretical investigations by Duke, Lipari, Salaneck, and Schein⁸ have not reproduced well the ultraviolet absorption spectrum of [2.2]paracyclophane. More recently, Wisor and Czuchajowski⁹ have interpreted this spectrum similarly to the early interpretations of Vala et al.⁶ and Iwata et al.²

The theoretical results of this paper are given in Table V and they are compared with the experimental values.² These calculations have been performed by using the structure determined through X-ray analysis by Hope, Bernstein, and Trueblood⁵ and distorted into a boat-like configuration with mean planes separated by 3.1 Å. The theoretical spectrum does not differ much from

(21) Birks, J. B.; Braga, C. L.; Lumb, M. D. *Proc. R. Soc.* **1965**, A283, 83.(22) Ron, A.; Schnepf, O. *J. Chem. Phys.* **1962**, 37, 2540.(23) Ron, A.; Schnepf, O. *J. Chem. Phys.* **1966**, 44, 19.

the idealized structure of two parallel *p*-xylenes with ring separation of 3.10 Å, as discussed before in subsection 3A. However, the calculated oscillator strengths are found here to be a sensitive function of the ring distortion.

The lowest observed band reported at 32 800 cm⁻¹ in solution has been determined to consist of two oppositely polarized bands lying very close in energy. In the single-crystal spectrum^{2,23} their origins are reported to lie at 30 360 and 30 740 cm⁻¹. The lower of these bands is observed to be γ (long axis) polarized, very weak (weaker than the forbidden ¹A_g-¹B_{2u} band of benzene), and possessing a long 236-cm⁻¹ progression. Only this lower state is reported to fluoresce and fluorescence is reported to be weak.²³

From our calculated results (Table V) we assign the first of these transitions as ¹B_{2g} (30 300 cm⁻¹) formally forbidden but borrowing intensity from a higher allowed ¹B_{2u} (40 300 cm⁻¹) state through an a_u vibration. The disorder necessary to produce this active vibrational mode has been observed in the crystal structure⁵ and in a thermodynamic study¹⁸ and it relates to a twisting of the rings in opposite directions about the major axis by about 3° each (see Figure 1). This vibration is held responsible for the observed spacings of 236 cm⁻¹ of the first band. This is in agreement with the interpretation of Vala et al.⁶ and may also apply to the theoretical results of Wisor and Czuchajowski,⁹ but their calculated lowest band (¹B_{2g} at 29 700 cm⁻¹) is perhaps too low compared to experiment (32 800 cm⁻¹). In fact there is a tendency in the theoretical results to overestimate the strong interaction between the two benzene rings in close proximity, producing an exaggerated lowering of the lowest ¹B_{2g} state. Figure 3 shows the very strong dependence of the calculated excitation energies upon variation of the interplanar separation. The second transition in this region we then assign to the ¹B_{3u} state calculated at 33 600 cm⁻¹.

The second absorption band is observed at 35 000 cm⁻¹ in solution. This transition has been assigned as ¹B_{3u}(x) by Vala et al.,⁵ but it has been observed by Iwata et al.² in the crystal spectrum to be very weak and to possess the characteristics of forbidden transitions with differently polarized vibrational structures. In this region we calculate a forbidden ¹B_{3g} at 36 000 cm⁻¹, which could borrow intensity from a higher ¹B_{2u} through the b_{1u} vibrational mode thus acquiring a γ polarization. This particular assignment of the second band would conform with the observations of Iwata et al.² and reconfirm our association of the first observed band to both ¹B_{2g} and ¹B_{3u}.

The third system, in the region 39 000–41 000 cm⁻¹, has been previously assigned by Vala et al.⁶ as ¹B_{2u}(γ). In good accord, we calculate a ¹B_{2u} state at 40 300 cm⁻¹. There are in fact two other calculated states in this region (¹B_{2g} at 40 300 cm⁻¹ and ¹B_{3g} at 42 400 cm⁻¹) and we would thus attribute the third band to these three excited states, but with most of the intensity of this system coming from the allowed ¹B_{2u} state with an oscillator strength of ~ 0.12 (γ). However, Iwata et al.⁶ report that this band appears as a clear peak in the polarized absorption spectrum, indicating x or z polarization instead. The lowest calculated z -polarized state is that at 46 800 cm⁻¹ (¹B_{1u}), which seems too high compared with the experimental region for this third band system, and also it is calculated to be very weak. This leaves the possibility of an x polarization. The ¹B_{3u} state calculated at 44 400 cm⁻¹ is more consistently attributed to the fourth band system, as we shall see, and therefore to be consistent with the experimentally reported polarization for the third band we conclude that either or both of the forbidden ¹B_{2g} (40 300 cm⁻¹) and ¹B_{3g} (42 500 cm⁻¹) borrow intensity from the ¹B_{3u} at 44 400 cm⁻¹ acquiring an x polarization via the b_{1u} or/and a_u vibrational mode (Figure 1).

The fourth band system is observed at 44 500 cm⁻¹. It is an intense band and possesses x or z polarization. In this region we have two allowed states, ¹B_{3u} at 44 400 cm⁻¹ and ¹B_{2u} at 45 200 cm⁻¹. The ¹B_{3u} has an x polarization and the assignment of this state as responsible for the fourth band would be consistent with both the intensity and the polarization of this fourth band system. Note that the ¹B_{1u} state at 46 800 cm⁻¹ has a z polarization and though weak may also contribute to this band.

The fifth band with x or z polarization is reported by Iwata et al.² at 48 700 cm⁻¹. This band may be easily assigned to the

Table VI. Nature of the Four Lowest Excited States of Di-*p*-xylene at Varying Inter-ring Separations and [2.2]Paracyclophane

state	transition ^a	xylene ^b	di- <i>p</i> -xylene			[2.2]para-cyclophane
			5.00 Å	3.73 Å	2.80 Å	
B _{2g}	d-e		0.56	0.65	0.79	0.83
	b-g		-0.45	-0.50	0.59	0.45
	c-f		0.55	0.44	-0.12	-0.26
	a-h		-0.44	-0.36	0.11	0.18
B _{3u}	d-f	0.57	0.55	0.59	0.70	0.67
	b-h	0.42	0.45	0.49	-0.63	-0.52
	c-e	0.57	0.54	0.50	-0.25	-0.45
	a-g	0.42	0.45	0.41	-0.22	-0.28
B _{3g}	d-g		0.66	0.89	0.95	0.98
	b-e		0.28	0.28	-0.30	-0.17
	c-h		-0.64	-0.33	0.01	0.08
	a-f		-0.27	-0.15	0.02	0.04
B _{2u}	d-h	0.64	0.63	0.77	0.89	0.96
	b-f	-0.29	-0.33	-0.49	0.44	0.23
	a-e	0.29	0.30	0.28	-0.06	-0.10
	c-g	-0.64	-0.62	-0.42	0.01	-0.09

^a Refer to the diagram for the characterization of the transition ^b Each coefficient has been divided by the square root of 2 for proper normalization and comparison with di-*p*-xylene.

Table VII. Calculated Triplet Spectrum of [2.2]Paracyclophane (All Energies are Given in 1000 cm⁻¹)

observed ^a energy	calculated		
	symmetry	absorption	emission
17.0–25.0	B _{3g}	30.3	15.8
	B _{2u}	33.6	
	B _{2g}	36.0	
	B _{3g}	40.3	
	B _{3u}	40.3	
	B _{2g}	42.4	

^a Reference 7; low-temperature emission in EPA.

strong ¹B_{3u} (x) state at 47 900 cm⁻¹ but there are several states calculated in this region ranging from the ¹B_{3g} at 47 400 cm⁻¹ to the ¹B_{1u} at 49 800 cm⁻¹, this latter having z polarization. The intense transition at 50 200 cm⁻¹ (¹B_{2u}) has more of the characteristics of the sixth band as we describe next.

Iwata et al.⁶ report the absorption spectrum of [2.2]paracyclophane up to 60 000 cm⁻¹. They find an intense sixth band with maximum at 53 000 cm⁻¹. A shoulder, the seventh band, is reported at 57 800 cm⁻¹. At 60 000 cm⁻¹ no evidence of absorption at higher energy is apparent. To conclude the interpretation of the absorption spectrum of [2.2]paracyclophane we address attention now to this strong band system at 53 000 cm⁻¹ and the shoulder at 57 800 cm⁻¹. The total oscillator strength of both of these systems is ~ 1.1 . The total calculated oscillator strength of all allowed bands between 50 000 and 60 000 cm⁻¹ is a factor of 2 too great.²⁴ With this indication it seems plausible to consider the calculated oscillator strength of each transition

(24) This is a characteristic feature of any singly excited CI treatment, however. Strong bands are calculated to have oscillator strengths about two times larger than observed experimentally when the dipole length operator is used for this purpose.

Table VIII. Comparison of Different Theoretical Models with Experiment for the Ionization Spectrum of [2.2]Paracyclophane (All Energies are Given in eV)^c

	INDO/S			ab initio		ref 10 DV-X	ref 25 exper.
	Koopmans ^a	Koopmans ^b	CI ₁	Koopmans ^a	SCF ^a		
b _{3g}	7.42	7.48	7.14	8.03	7.35	8.14	8.1
b _{2g}	8.11	7.96	8.00	8.16	7.51	8.17	8.1
b _{2u}	8.48	9.17	8.30	8.79	8.19	8.56	8.4
b _{3u}	10.00	9.98	9.72	10.01	9.41	9.55	9.6
b _{1u}	10.11	10.97	9.87	11.68	11.17	10.19	10.3

^aThis work with the experimental geometry. ^bThis work with geometry of di-*p*-xylene with inter-ring separation of 3.1 Å. ^cOur calculations utilize the crystallographic structure, except where noted.

as nearly twice as intense as it should be, for distributing the great number of theoretically calculated states in the region corresponding to the sixth and seventh band systems. Accordingly, the sixth band would be composed by those states ranging from the intense ¹B_{2u} at 50 200 cm⁻¹ to the ¹B_{3u} at 57 100 cm⁻¹ or ¹A_g at 57 500 cm⁻¹. The shoulder at 57 800 cm⁻¹ we assign to several transitions including the allowed ¹B_{2u} states (58 800 cm⁻¹) and ¹B_{1u} (59 500 cm⁻¹) states. After 60 000 cm⁻¹ there is very little intensity, in agreement with the rapidly decreasing absorption apparent at 60 000 cm⁻¹. We do not report any transitions lying above ~60 000 cm⁻¹ where experimental information is not available and the theoretical values are more uncertain.

In Table VI the nature of the four most interesting excited states is examined. At the interplanar separation of 5.0 Å these excitations are very similar to those of xylene itself (see also Figure 2). For the [2.2]paracyclophane the lowest excited state, of ¹B_{2g} symmetry, is strongly delocalized, and represents the promotion of an electron from a ring-to-ring antibonding orbital into one of bonding nature. This decreases the ring separation of this ¹B_{2g}, as compared to the ground state ¹A_g, by as much as 0.31 Å.¹¹ Also it increases the bond order between the π systems considerably. The ¹B_{3g} is similar but contains less excimer contribution (is more delocalized). The ¹B_{3u} and ¹B_{2u} states are calculated to have little effect on the ring-to-ring bond order and little consequence on the interring separation. The ¹B_{3u} exhibits excimer character (superposition of localized xylenes excitations), whereas the ¹B_{2u} is delocalized.

E. Triplet Spectrum of [2.2]Paracyclophane. The calculated triplet spectrum of the [2.2]paracyclophane is shown in Table VII. The lowest energy transition is calculated as ³B_{3g} at 30 300 cm⁻¹. This state corresponds to the spatially forbidden component of the *y*-allowed second singlet band in xylene. The ³B_{2g}, corresponding to the lowest singlet, is calculated as the third triplet in a fashion analogous to that found in benzene itself.

Hillier, Glass, and Rice⁷ report the low-temperature emission spectrum of [2.2]paracyclophane in EPA. The phosphorescence spectrum is very broad, ranging from ~17 000 to ~25 000 cm⁻¹. The estimated⁷ 0-0 band at 25 000 cm⁻¹ corresponds to a shift of ~5000 cm⁻¹ from that of benzene. At the Franck-Condon region of the ¹A_g ground state we calculate the lowest ³B_{3g} at 30 300 cm⁻¹. This value seems too high compared to the experimental result. However, it may be noted that emissions take place in the Franck-Condon region of the excited states. For ³B_{3g} the most important configuration is the one corresponding to the promotion b_{3g}-a_g, thus involving a transition from an orbital that is antibonding (b_{3g}) into another that is bonding (a_g) with respect to the ring-to-ring interaction. Therefore, the equilibrium inter-ring separation for the ³B_{3g} state should be shorter than that for the ¹A_g ground state accounting for the calculated value for the transition energy into this triplet state as being larger than the experimental value for the emission. For instance,¹¹ the triplet B_{3g} excited state is calculated to have an inter-ring separation that is 0.2 Å shorter compared to the ground state ¹A_g. Utilizing the ab initio result¹¹ obtained for the geometry of the excited ³B_{3g} state the emission to the ground-state ¹A_g is calculated as 15 800 cm⁻¹ in good agreement with the origin of the phosphorescence spectrum⁷ at ~17 000 cm⁻¹.

F. The Photoelectron Spectrum of [2.2]Paracyclophane. The photoelectron spectrum of [2.2]paracyclophane gives additional information of the magnitude of the interaction between the

inter-ring π-electron systems. This spectrum has been recorded several²⁵ times and Kovac et al.²⁶ give a very detailed and comprehensive account for the He Iα region. In this region five ionization peaks are attributed to ionization out of the five outermost occupied molecular orbitals of [2.2]paracyclophane. A review by Heilbronner and Yang²⁷ summarizes the early theoretical efforts. More recently, Doris et al.¹⁰ have undertaken theoretical studies using the discrete variational Hartree-Fock-Slater (DV-Xα) method. Their results are in very good agreement with the experimental ionization energies, particularly regarding the unobserved splitting of the two lowest π levels.

In this paper we report results obtained at both the semi-empirical INDO/S scheme, as adopted throughout this paper, as well as the ab initio SCF level, using the GAMESS program.¹⁶ The INDO/S calculations are performed at the crystallographic structure⁵ and utilize the CI model with excitations generated from the ²B_{3g} state of the cation. This scheme has been successfully applied in previous studies²⁸ and is capable of describing satellite lines (though none is expected nor calculated to occur in the He Iα region of [2.2]paracyclophane). The ab initio SCF calculations are made at the optimized theoretical geometry¹¹ and employ the basis set of Dunning and Hay¹⁷ (9s5p/4s) contracted to split-valence (3s2p/2s). For reference, the ground-state SCF energy is calculated as -614.9802 au and the theoretically calculated geometry has the boat-like distortion observed experimentally, with an inter-ring separation of 3.07 Å compared to the crystallographic value of 3.10 Å.

The results obtained for the first five ionization potentials are given in Table VIII and are compared with the theoretical DV-Xα results of Doris et al.¹⁰ and the experimental values of Kovac et al.²⁶ The INDO/S results obtained at the Koopmans levels of approximation show a separation of 0.7 eV for the first two ionizations, compared to the near degeneracy reported experimentally. For comparison, we also show the Koopmans values for the idealized structure of di-*p*-xylene with planar rings separated by 3.10 Å. It is to be noted that this splitting is now slightly reduced, indicating the influence of boat-like distortion on the splitting of the first two π ionizations.

The electronic absorption spectrum of the radical cation of [2.2]paracyclophane has been obtained and analyzed by Badger and Brocklehurst²⁹ and it is also appropriate for the comparison with our CI INDO/S results, which involve a CI calculation out of the ²B_{3g} ground state of the cation. The spectrum of the cation of [2.2]paracyclophane²⁹ in a matrix of *n*-butyl chloride/isopentane at 77 K shows a strong first band with maximum at ~1.1 eV. This could be assigned to the ²B_{3g}-²B_{2g} transition calculated at 0.9 eV, resulting in some discrepancy in the interpretation of the

(25) (a) Boekelheide, V.; Schmidt, W. *Chem. Phys. Lett.* **1972**, *17*, 410. (b) Pignataro, S.; Mancini, V.; Ridyard, J. N. A.; Lemka, H. J. *Chem. Commun.* **1971**, 142. (c) Boschi, R.; Schmidt, W. *Angew. Chem., Int. Ed. Engl.* **1971**, *12*, 402. (d) Heilbronner, E.; Maier, J. P. *Helv. Chim. Acta.* **1974**, *57*, 151. (e) Koenig, T.; Wielesek, R. A.; Snell, W.; Balle, T. *J. Am. Chem. Soc.* **1975**, *97*, 3225.

(26) Kovac, B.; Mohraz, M.; Heilbronner, E.; Boekelheide, V.; Hopf, H. *J. Am. Chem. Soc.* **1980**, *102*, 4314.

(27) Heilbronner, E.; Yang, Z. Z. *Top. Curr. Chem.* **1983**, *115*, 1.

(28) (a) Anderson, W. P.; Edwards, W. D.; Zerner, M. C.; Canuto, S. *Chem. Phys. Lett.* **1982**, *88*, 185. (b) Edwards, W. D.; Zerner, M. C. *Int. J. Quantum Chem.* **1983**, *23*, 1407.

(29) Badger, B.; Brocklehurst, B. *Trans. Faraday Soc.* **1969**, *65*, 2582; **1970**, *66*, 2939.

ionization spectrum which suggest this splitting is quite small. The observed nature of this peak, however, suggests an allowed band and our ${}^2B_{3g} \rightarrow {}^2B_{3u}$ transition calculated at 1.2 eV seems a better candidate. Another strong peak is observed at 2.4 eV. This we would assign to the ${}^2B_{3g} \rightarrow {}^2B_{1u}$ transition calculated at 2.7 eV. Two weak peaks are observed at about 1.7, and 2.1 eV. The peak at 1.7 eV may be due to impurities^{27,29} while that at 2.1 eV might be assigned with the forbidden ${}^2B_{3g} \rightarrow {}^2B_{2u}$ transition calculated at 2.6 eV. Although these assignments of the spectrum of the cation seem reasonable, we remark that the geometry of the cation is somewhat different from that of the neutral¹¹ and the photoelectron spectrum of Table VIII is calculated at the geometry of the neutral.

The ab initio results show the near absence of the splitting of the b_{3g} and b_{2g} π ionization, but the ionization values are more successfully described at the Koopmans level. It is expected that inclusion of correlated corrections will improve further the ab initio results. This is however a great computational task and it should be emphasized that the nature of [2.2]paracyclophane may require the inclusion of higher levels of excited configurations to help to restore some of the local nature of each ring, perhaps requiring quadruple excitations with respect to the ground neutral state.

The INDO/S results for the $(b_{3g})^{-1}$ state seem systematically lower than the experimental first ionization potential, indicating too strong an interaction between the rings. Decreasing such an interaction would have an effect also in the calculated absorption spectrum. It would of course have no effect on xylene (where the agreement between the theoretical and experimental results is excellent), but it would increase the first excitation energy of the [2.2]paracyclophane. This would give an even better agreement between the experimental and calculated values for the transition energies and corroborates the interpretation of the absorption spectrum of [2.2], [3.3], [4.4], and higher order paracyclophanes as presented in this paper. Of interest is that all methods examined here give the same ordering of states, not necessarily an easy task given the crossing of states suggested in Figure 2.³⁰

4. Summary

The INDO/S method has been used to help examine the spectroscopy of the [*n*.*n*]paracyclophanes. For *n* > 3 the calcu-

lations indicate only a doubling of the xylene bands, as might be expected for weakly interacting dimers. The predicted spectra for these paracyclophanes are then similar to that of xylene itself, in agreement with experiment.

The [3.3]paracyclophane has a spectrum that is considerably different from that of the higher analogues. The first band observed in absorption is assigned to the second calculated state, the allowed ${}^1B_{3u}$, but with the first calculated state, ${}^1B_{2g}$, borrowing intensity from higher states. This assignment is in good agreement with the experimental information and the lowest calculated state may also be apparent as an inflection on the first observed band, and it is held responsible for the emission observed in concentrated benzene solution with interplanar separation similar to that found in [3.3]paracyclophane.

The spectrum of [2.2]paracyclophane is more complex. A detailed analysis of the theoretical results and comparison with the experimental absorption spectrum has been performed. A very satisfactory assignment has been presented that conforms with all known experimental characteristics. We believe that the interpretation put forward in this paper is the most consistent so far available. The lowest band consists of two transitions, one allowed (${}^1B_{2u}$) and the other (${}^1B_{2g}$) borrowing intensity from a higher ${}^1B_{2u}$ state via the a_u vibrational mode. The second band is mainly due to the transition to the ${}^1B_{2u}$ state having *y* polarization. The lowest excited state, ${}^1B_{2g}$, is the one responsible for the weak fluorescence and for the long axis (*y*) polarized absorption. The observed phosphorescence of the [2.2]paracyclophane is assigned to the emission ${}^3B_{3g} \rightarrow {}^1A_g$ and it has been calculated an ab initio SCF geometry optimization of this triplet excited state.

The calculation of the He I α ionization spectrum of [2.2]-paracyclophane has also been made and it is in good agreement with experiment, particularly for the more energetic of the first five known bands. The results are in agreement with the experimental assignment,²⁵ whether we consider the ab initio SCF or INDO/S calculations.

Acknowledgment. S.C. is grateful to the hospitality of the Quantum Theory Project at the University of Florida. This work was supported in part through grants from the National Research Council of Brazil (CNPq), The National Science and Engineering Research Council of Canada, Eastern Kodak Company, and the College of Liberal Arts and Sciences at the University of Florida.

(30) See, however, the CNDO results of ref 8.